Characterization of complementary electric field coupled resonant surfaces

Thomas H. Hand,[a] Jonah Gollub, Soji Sajuyigbe, David R. Smith, and Steven A. Cummer
Center for Metamaterials and Integrated Plasmonics, Department of Electrical Engineering, Duke University, Durham, North Carolina 27708, USA

(Received 2 October 2008; accepted 6 November 2008; published online 26 November 2008)

We present angle-resolved free-space transmission and reflection measurements of a surface composed of complementary electric inductive-capacitive (CELC) resonators. By measuring the reflection and transmission coefficients of a CELC surface with different polarizations and particle orientations, we show that the CELC only responds to in-plane magnetic fields. This confirms the Babinet particle duality between the CELC and its complement, the electric field coupled LC resonator. Characterization of the CELC structure serves to expand the current library of resonant elements metamaterial designers can draw upon to make unique materials and surfaces. © *2008 American Institute of Physics*. [DOI: 10.1063/1.3037215]

Engineered structures called metamaterials exhibit electric and magnetic responses not found in conventional materials, such as negative refraction.[1] The geometry and structure of metamaterials can be engineered to achieve a wide spectrum of electromagnetic responses, in contrast to conventional materials that gain their electromagnetic properties through their material composition. To achieve exotic responses, metamaterials typically consist of dielectrics and conductors shaped in various geometries to couple to the electric and magnetic field components of an electromagnetic wave, which set up artificial dipole moments in the material. Metamaterials can be divided into two categories: bulk structures and surfaces. Two well known particles, the split-ring resonator (SRR)[2] and the electric field coupled inductive-capacitive (ELC)[3] resonator are examples of bulk metamaterials. Typically arranged in a three dimensional matrix, they form a material that possesses a finite thickness through which the definition of an effective refractive index n has meaning. In contrast, metamaterial surfaces ideally have zero thickness in the propagation direction, and thus the interpretation of an effective surface impedance is more appropriate. Metamaterial surfaces are of considerable interest since they can be used in either a waveguide[4–6] or a free-space regime. The complementary SRR (CSRR) has been analyzed using Babinet's principle.[4] It was shown to be resonant when excited by a wave with an electric field component normal to the surface. The CSRR has been shown to be useful in the waveguide environment, where it was used to demonstrate electromagnetic tunneling through a channel.[6]

In this paper, we focus our attention on characterizing the magnetic counterpart of the CSRR, the complementary electric LC (CELC) resonator. Its complement, the ELC resonator, exhibits a purely electric response with no magnetoelectric coupling.[3] It is of interest to verify that the CELC achieves a purely magnetic response with no cross coupling. The CELC metamaterial structure offers potential applications in both free-space and waveguide environments similar to the CSRR, which was shown to realize passive phase shifters,[7] filters,[5,8,9] power splitters,[10] etc.

The duality between the CELC and the ELC can be understood by applying Babinet's principle. If an infinite sheet in the $z=0$ plane composed of resonant ELCs is illuminated by some incident fields $\mathbf{E}^0$ and $\mathbf{H}^0$ (propagating in the $+z$-direction) and its complement (the CELC) is illuminated by the $+z$ traveling incident fields $\mathbf{E}_c^0$ and $\mathbf{H}_c^0$, then Babinet's principle requires that[4,11,12]

$$\mathbf{E}_c^0 = \mathbf{E}_c - Z_0\mathbf{H}, \quad \mathbf{H}_c^0 = \mathbf{H}_c + (1/Z_0)\mathbf{E} \tag{1}$$

be satisfied for $z>0$, where $Z_0=\sqrt{\mu_0/\epsilon_0}\approx 377\ \Omega$ and $\mathbf{E}$, $\mathbf{H}$ and $\mathbf{E}_c$, $\mathbf{H}_c$ are the total fields for the ELC and CELC systems, respectively. The incident fields are related to each other by[12,13] $\mathbf{E}^0=Z_0\mathbf{H}_c^0$ and $\mathbf{H}^0=-(1/Z_0)\mathbf{E}_c^0$. Since all of the currents are confined in the $z=0$ plane, the scattered fields $\mathbf{E}'$, $\mathbf{H}'$ and $\mathbf{E}_c$, $\mathbf{H}_c$ must have certain symmetries in z: H_z', E_x', and E_y' are even functions of z, while E_z', H_x', and H_y' are odd functions.[4,11] Using the Babinet principle, if an ELC is excited by an incident plane wave with polarization $\mathbf{E}_0=\hat{\mathbf{x}}E_0$, then the ELC will generate an electric dipole $\mathbf{p}\propto\mathbf{E}^0$, and the scattered fields $\mathbf{E}'$ and $\mathbf{H}'$ are approximately the fields generated by $\mathbf{p}$. There is no net magnetic dipole $\mathbf{m}$ for the ELC due to the oppositely wound inductive loops.[3] Because of the even symmetry requirement on E_x', $\mathbf{p}$ does not change signs across $z=0$. In order to satisfy Eq. (1), the fields scattered by the CELC for $z>0$ $(\mathbf{E}_c', \mathbf{H}_c')$ should be those produced by a magnetic dipole $\mathbf{m}\propto\mathbf{H}_c^0$. $\mathbf{E}_c^0=-Z_0\mathbf{H}^0$ implies that $\mathbf{E}^0$ incident on the ELC must be rotated 90° around the propagation axis in order to excite the CELC. Because of the odd symmetry requirement on H_x', $\mathbf{m}$ must change sign across across $z=0$. An intuitive physical understanding of how the CELC is excited by an incident magnetic field is difficult, but rigorous application of the Babinet principle shows clearly the dual responses of complementary particles.

Figure 1 shows a full wave simulation (using Ansoft HFSS™) of the vector electric and magnetic fields in the $y=0$ plane for the ELC and CELC particles, respectively. These simulations confirm the required symmetry of the fields as discussed above. Also shown in Fig. 1 (bottom right) is the current density on the CELC surface at resonance. From Babinet's principle, we know that this current is induced by the magnetic field component $(\hat{\mathbf{x}}H_x)$ of the incident wave normal to the gap complement (the dielectric region in the CELC complementary to the capacitive plates of the ELC).

[a]Electronic mail: thh5@duke.edu.

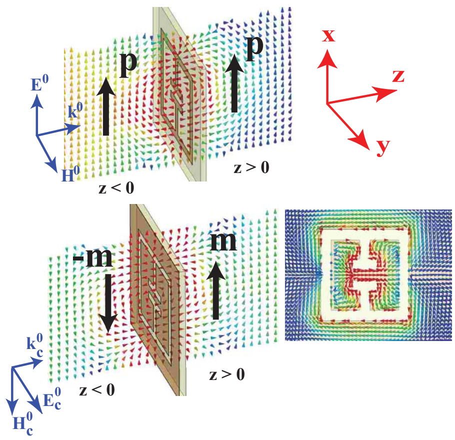

FIG. 1. (Color online) Ansoft HFSS™ simulation of the vector ELC electric field (top) and CELC magnetic field (bottom) (in the $y=0$ plane) when illuminated by an incident electromagnetic plane wave from $z<0$. The bolded arrows show the direction of the dipoles [with $\exp(+j\omega t)$ implied]. Notice that for the CELC, the sign of the magnetic dipole $\mathbf{m}$ changes sign from $z<0$ to $z>0$ due to the odd symmetry requirement on H_x'. Shown in the bottom right is a simulation showing the current mode generated by the CELC at resonance.

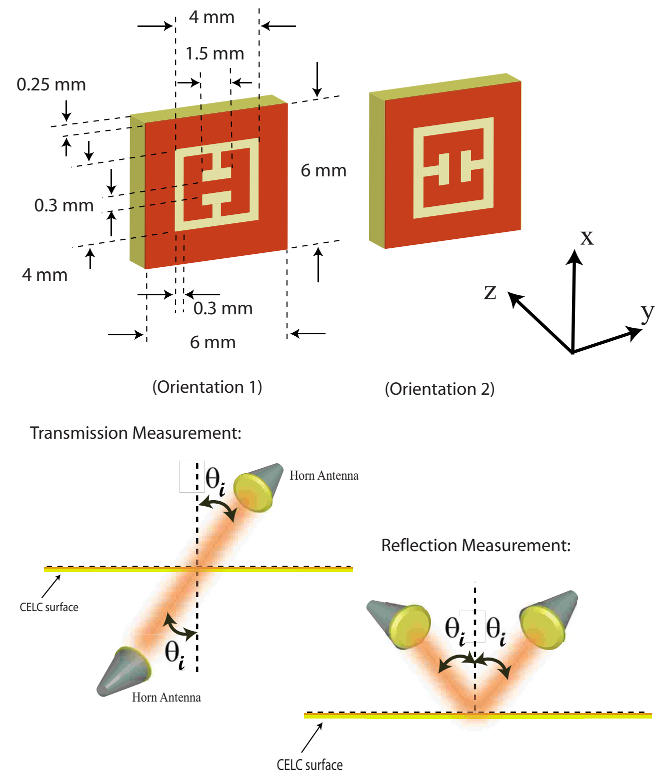

FIG. 2. (Color online) Top left: Illustration of the designed CELC particle with orientation 1. Top right: same dimensions as the design to its right, with the CELC pattern rotated 90° (orientation 2). Bottom left: Diagram showing how transmission measurements were made. Bottom right: Diagram showing how reflection measurements were made.

To determine the complete electromagnetic behavior of the CELC, we fabricated two arrays of CELC particles. The second sheet was identical to the first sheet except that the CELC patterns were rotated by 90°. By measuring the transmission and reflection coefficients of the two sheets for transverse electric (TE) and transverse magnetic (TM) polarized waves over a range of angles, we can determine the field configurations necessary to excite a resonance. The CELC unit cell was designed to be resonant in the *X*-band (8–12 GHz) due to the convenience of free-space measurements in this range. A close-up view of the particle (designed for a resonance near 10.5 GHz) with marked dimensions is shown in Fig. 2. Dielectric lens antennas (1 ft focal length) were used to make measurements of the transmitted and reflected fields. The fabricated CELC surfaces were placed halfway between the transmitter and receiver, where a rotating stage was used to turn the lens antennas so that the reflected and transmitted fields could be measured over various angles. All measured data were taken using an Agilent N5230A network analyzer. The CELC surfaces were fabricated on a 250 μm thick FR4 board with a copper trace thickness of 17 μm using standard photolithography. The boards measured 15.24×15.24 cm^2 with a unit cell size of 6×6 mm^2.

Figure 3 shows the reflection and transmission coefficient magnitudes of the CELC surface in orientation 1 for TE and TM incidence over angles ranging from 0° to 60° degrees. Transmission was measured from 0° to 60°, and reflection was measured from 30° to 60°. Consistent with our expectation, we observe no resonance excitation for orientation 1 with TE polarization (Fig. 3, bottom row). This is expected since no matter the angle of incidence, no magnetic field component is ever perpendicular to the gap complement. Notice that the reflection coefficient is near unity and the transmission coefficient is suppressed, indicating that the sheet behaves as a conducting surface for this polarization and particle orientation.

The top row of Fig. 3 shows the reflection and transmission of the CELC surface for orientation 1 with TM polarization. In this configuration, the magnetic field is always perpendicular to the gap complement of the CELC no matter what the angle of incidence. The magnetic field energy in the wave induces current in the *y*-direction, which drives the resonance. The magnitude of this induced current is proportional to the incident magnetic field $\mathbf{H}^0=\hat{\mathbf{x}}H^0$, which is invariant to the incidence angle. This is the reason why the strength of the resonance is relatively unchanged with inci-

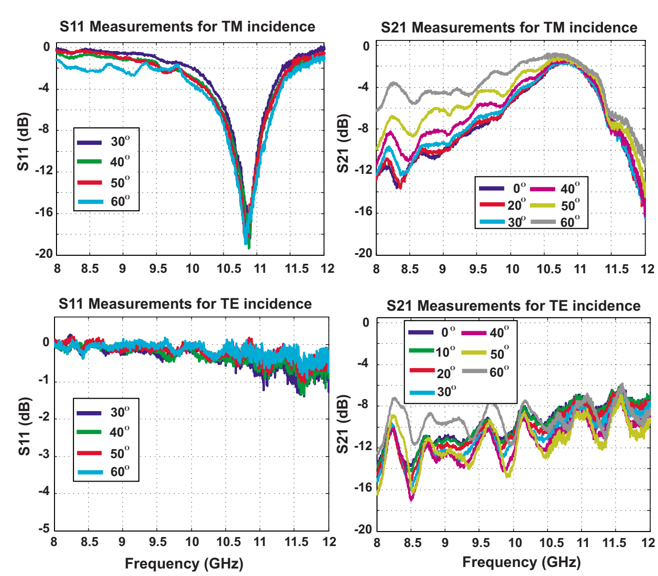

FIG. 3. (Color online) Measurements for the CELC sheet in orientation 1. Top row: S_{11} measurements (left) and S_{21} measurements (right) over several incidence angles for TM polarization ($\mathbf{H}^0=\hat{\mathbf{x}}H^0$). Bottom row: S_{11} measurements (left) and S_{21} measurements (right) over several incidence angles for TE polarization ($\mathbf{E}^0=\hat{\mathbf{x}}E^0$).

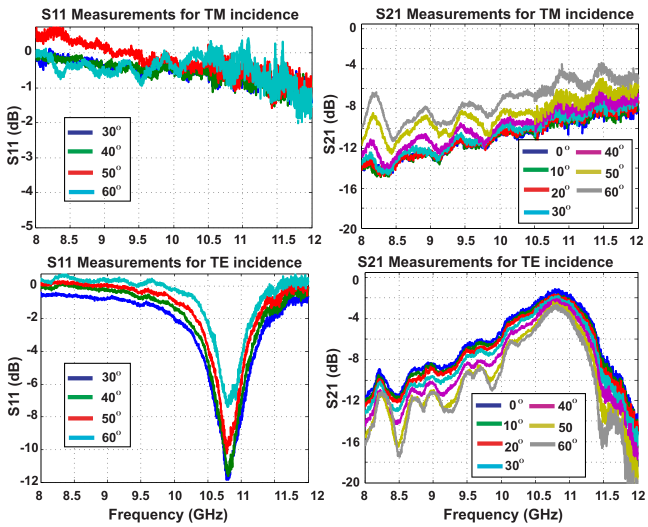

FIG. 4. (Color online) Measurements for the CELC sheet in orientation 2. Top row: S_{11} measurements (left) and S_{21} measurements (right) over several incidence angles for TM polarization ($\mathbf{H}^0 = \hat{\mathbf{x}} H^0$). Bottom row: S_{11} measurements (left) and S_{21} measurements (right) over several incidence angles for TE polarization ($\mathbf{E}^0 = \hat{\mathbf{x}} E^0$).

dence angle. An argument as to why the electric field does not excite the resonance in the CELC is because as the angle of incidence increases, the component parallel to the gap complement E_y decreases. If it were the electric field that was responsible for driving the resonance, then the response should weaken as the incidence angle increases, which is clearly not the case. It can be seen from Fig. 3 for TM incidence that the transmission becomes slightly enhanced for large incident angles. This is due to the fact that for large incident angles, the effective area of the CELC surface with respect to the lens antennas decreases; thus, less of the incident energy interacts with the metamaterial surface. This same effect is also noticeable for TE incidence (Fig. 3), where the sheet behaves as a conducting surface.

Figure 4 shows the TE and TM reflection and transmission magnitudes for orientation 2. For TE incidence, it is clear that at normal incidence the magnetic field is completely normal to the gap complement and parallel to the surface ($H_z = 0$). Thus, we expect the particle to couple strongly to this wave. The resonance in the reflection coefficient weakens for waves away from normal incidence, an expected result since H_z increases and the parallel component H_y normal to the CELC gap complement diminishes as the angle of incidence increases. The transmission at resonance also decreases with large angles of incidence due to weaker magnetic coupling. Figure 4 (top row) shows the response of the CELC sheet in orientation 2 with TM polarization. As can be seen, there is no incidence angle with a component of the magnetic field normal to the CELC gap complement, resulting in no resonance excitation. For this particle orientation and incidence polarization, the surface behaves like a flat conducting sheet (equivalent to orientation 1 for TE polarization). Full wave simulations of the different particle orientations with TE and TM incidence (not shown) were executed using Ansoft HFSS™, and the results closely agreed with the measurements of Figs. 3 and 4.

In summary, the transmission and reflection coefficients of CELC surfaces were measured to show that the particle can only be excited when illuminated with an in-plane magnetic field perpendicular to the gap complement, consistent with the Babinet principle and full wave simulations. This study shows that frequency selective surfaces can be designed that have a response only to magnetic fields. By characterizing the CELC, we have expanded the current library of metamaterial structures, and we have shown how the CELC can be used as a frequency selective surface or in a waveguide environment.

[1]D. R. Smith, W. Padilla, D. Vier, S. Nemat-Nasser, and S. Schultz, Phys. Rev. Lett. **84**, 4184 (2000).
[2]J. Pendry, A. Holden, D. Robbins, and W. Stewart, IEEE Trans. Microwave Theory Tech. **47**, 2075 (1999).
[3]D. Schurig, J. Mock, and D. R. Smith, Appl. Phys. Lett. **88**, 041109 (2006).
[4]F. Falcone, T. Lopetegi, M. Laso, J. Baena, J. Bonache, M. Beruete, R. Marqués, F. Martín, and M. Sorolla, Phys. Rev. Lett. **93**, 197401 (2004).
[5]F. Falcone, T. Lopetegi, J. Baena, R. Marqués, F. Martín, and M. Sorolla, IEEE Microw. Wirel. Compon. Lett. **14**, 280 (2004).
[6]R. Liu, Q. Cheng, T. Hand, J. Mock, T. Cui, S. A. Cummer, and D. R. Smith, Phys. Rev. Lett. **100**, 023903 (2008).
[7]M. Antoniades and G. Eleftheriades, IEEE Antennas Wireless Propag. Lett. **2**, 103 (2003).
[8]J. Garcia-Garcia, F. Martin, F. Falcone, J. Bonache, I. Gil, T. Lopetegi, M. Laso, M. Sorolla, and R. Marques, IEEE Microw. Wirel. Compon. Lett. **14**, 416 (2004).
[9]C. Caloz and T. Itoh, IEEE Trans. Antennas Propag. **52**, 1159 (2004).
[10]M. Antoniades and G. Eleftheriades, IEEE Microw. Wirel. Compon. Lett., **11**, 808 (2005).
[11]J. D. Jackson, *Classical Electrodynamics*, 3rd ed. (Wiley, New York, 1999).
[12]H. T. Chen, J. F. O'Hara, A. J. Taylor, R. D. Averitt, C. Highstrete, M. Lee, and W. J. Padilla, Opt. Express **15**, 1084 (2007).
[13]J. A. Kong, *Electromagnetic Wave Theory*, 2nd ed. (Wiley, New York, 1990).